Engineering Notes

Sliding-Mode Control Strategies for Rendezvous and Docking Maneuvers

Elisa Capello,* Elisabetta Punta,† Fabrizio Dabbene,†
Giorgio Guglieri,‡ and Roberto Tempo†
CNR-IEIIT, Politecnico di Torino, 10129 Torino, Italy

DOI: 10.2514/1.G001882

I. Introduction

RENDEZVOUS and docking maneuvers represent operational key technologies in many spacecraft missions and consist of a series of orbital maneuvers and controlled trajectories during which an active spacecraft (chaser) tries to capture a passive target vehicle. The goal of the mission is that the chaser vehicle has to safely and efficiently approach, up to few centimeters (surface-to-surface), the target vehicle, satisfying the strict requirements of docking in terms of relative position, speed, and with zero angular velocities. Once the target is reached, the chaser has to remain stationary until the hold mechanism captures and docks the target vehicle. The faced problem requires control of both the relative position and the relative attitude of the vehicles.

Our focus is on the final approaching phase of the rendezvous maneuver, which is considered to start when the chaser is 500 m far from the target. The aim of the control strategy is twofold: 1) the controller must guarantee that the chaser tracks the specified position of the target while 2) the attitude stability is maintained. These goals must be reached despite the environmental disturbances acting on the spacecraft and taking into account the uncertainties affecting the actuators: the performances of which are subject to physical constraints related to their feasible switching frequency and intensity of the thrusts.

The novelty of the proposed approach is detailed in the following. First, it is shown how one can take advantage of the discontinuous control signals produced by first-order sliding-mode control (SMC), which are typically seen as an undesirable behavior, to design a tracking control able to efficiently cope with the switching nature of the thrusters. This leads to a control strategy which is 1) simple to implement because it translates immediately into a flight compliant algorithm with minimum computational power (see Algorithm 1 in Sec. III.B); and 2) fuel-efficient because the simulations presented in this Note show how the fuel consumption is, by far, inside the limits required by actual technology. Indeed, fuel consumption reduction is one of the driving objectives of our study: it is shown how the designed SMC achieves good position and velocity tracking while guaranteeing a limited consumption. To achieve this, the developed first-order SMC is also shown to perform satisfactorily when implemented at a rather low frequency. This represents a clear advantage because it decreases the interval time when the thruster is switched on. In general, the use of SMC for thruster control has been discouraged (see, for instance, [1]) because it is deemed to lead to excessive fuel consumption, due to switching on/off thrusters at high frequency. Indeed, a good performance of the sliding-mode controller has to usually be traded off for significant fuel usage. This drawback is countered in our approach.

Second, the robustness of SMC is exploited to design a controller for a realistic model, in which complete spacecraft dynamics and kinematics are considered, including actuator nonlinearities and saturations. Moreover, our analysis and simulation take into specific account the presence of external environment disturbances.

Concerning the attitude stabilization, it should be remarked that it represents a problem of particular importance for spacecraft because it is fundamental for enforcing precision and for guidance, as short propulsive maneuvers must be executed with extremely accurate alignment [2]. The phase of approaching involves highly nonlinear kinematics and dynamics. Hence, linear control methodologies appear to not be suitable for this application. Different advanced control techniques have been proposed in the literature, including H_∞ control [3], Riccati equation techniques [4], $\theta - D$ nonlinear optimal control techniques [5], feedback-linearization-based approaches [6], and model predictive control [7]. Even if a nonlinear model of spacecraft orbital motion and cone constraints is usually considered in the literature, these approaches are limited to constant attitude variations and no external environment disturbances are analyzed. In our proposed approach, as previously explained, we consider a detailed six-degree-of-freedom dynamic model, actuator nonlinearities, and disturbances to develop a two-channel SMC.

Interesting applications of SMC have been proposed for spacecraft position or attitude control due to their ability to guarantee both accuracy and robustness. SMC (see [8]) is a nonlinear control approach, which provides global stability and ensures insensitivity and robustness to system uncertainties and external disturbances under rather mild assumptions. First-order sliding-mode controllers are discontinuous and depend on suitably designed switching functions. Second-order sliding-mode strategies were subsequently introduced with the aim of reaching the sliding manifold in finite time by means of continuous control (i.e., chattering reduction) [9,10]. Good performance and applications of both first- and second-order sliding-mode strategies for aerospace vehicles can be found in the literature (see [11,12]). In [13], two robust sliding-mode controllers for position and attitude tracking of spacecraft subject to external disturbances are analyzed. However, the actuator system and the position dynamics for a real spacecraft are not deployed.

The contribution of this work is the design of two controllers: 1) a first-order SMC for position tracking and 2) a supertwisting (STW) second-order SMC for attitude stability, in which the mutual influence is taken into account by the introduction of additional disturbances. Key features of the developed control approach and the feasibility of the proposed design are in terms of 1) fuel consumption, 2) robustness to model uncertainty and exogenous disturbances, and 3) fault tolerance. Extensive simulations on a very detailed nonlinear model have been carried out to validate the performance of the proposed SMC design.

This Note is organized as follows. In Sec. II, a detailed spacecraft model is analyzed, including actuator models, position and attitude dynamics, and external disturbances. The proposed SMC strategies are developed in Sec. III. The simulation results are in Sec. IV. Conclusions are drawn in Sec. V.

Received 30 November 2015; revision received 14 November 2016; accepted for publication 14 November 2016; published online 30 January 2017.

*Department of Mechanical and Aerospace Engineering, Corso Duca degli Abruzzi 24; National Research Council of Italy, Institute of Electronics, Computer and Telecommunication Engineering.

†National Research Council of Italy, Institute of Electronics, Computer and Telecommunication Engineering, Corso Duca degli Abruzzi 24.

‡Department of Mechanical and Aerospace Engineering, Corso Duca degli Abruzzi 24.

II. Spacecraft Model

This section describes in detail the spacecraft model considered in our work.

A. Actuator Models

The actuation system is composed of 12 thrusters (see Fig. 1), the task of which is to translate the on/off command computed by the controller into thrust and moment variations, according to their shoot direction and their location with respect to the center of mass (COM) position, and they cannot be modulated. A zero nominal moment is guaranteed with the definition of thrusters position as in Fig. 1. A model for the errors is defined for the thrusters including bias and random error components [14,15].

To model the different sources of uncertainty, the total thruster force of the ith thruster is described as

$$F_{\text{thr}_i} = \beta_i T_{\text{mag}_i} d_{\text{thr}_i}, \qquad i = 1, \ldots, N_{\text{thr}} \tag{1}$$

with $N_{\text{thr}} = 12$ as the total number of thrusters. The vector $\beta \in \mathbb{R}^{N_{\text{thr}}}$ is a Boolean vector related to the thruster switching on/off. The magnitude $T_{\text{mag}_i} \in \mathbb{R}$ of the force applied by the ith thruster is modeled as

$$T_{\text{mag}_i} = T_{\max} + \Delta T_{\text{mag}_i}$$

with $T_{\max} \in \mathbb{R}$ as the maximum thrust produced by each single thruster, and $\Delta T_{\text{mag}_i} \in \mathbb{R}$ as the error in the magnitude of the force applied by ith thruster. The vector $d_{\text{thr}_i} \in \mathbb{R}^3$ is the vector representing the shoot direction of the ith thruster; that is,

$$d_{\text{thr}_i} = d^0_{\text{thr}_i} + \Delta d_{\text{thr}_i}$$

where $d^0_{\text{thr}_i} \in \mathbb{R}^3$ is the vector of the nominal shoot direction, defined by considering the thruster scheme of Fig. 1; and $\Delta d_{\text{thr}_i} \in \mathbb{R}^3$ is the shooting direction error due to nonperfect assembly. Hence, the nominal force applied by each thruster can be written as

$$F^0_{\text{thr}_i} = \beta_i T_{\max} d^0_{\text{thr}_i}$$

corresponding to the ideal case in which no errors on the magnitude and shoot direction are considered, and the resulting total force applied by thrusters is given by

$$F_{\text{thr}} = \sum_{i=1}^{N_{\text{thr}}} F_{\text{thr}_i} \tag{2}$$

The total moment due to the thrusters is evaluated as

$$M_{\text{thr}} = \sum_{i=1}^{N_{\text{thr}}} F_{\text{thr}_i} \times \ell_i$$

where $\ell_i \in \mathbb{R}^3$ is the ith thruster position vector for $i = 1, \ldots, N_{\text{thr}}$. The vector ℓ_i changes during the maneuver as

$$\ell_i = \ell^0_i + \Delta\ell_i$$

where $\ell^0_i \in \mathbb{R}^3$ represents the vector of initial position of the thrusters, and $\Delta\ell_i \in \mathbb{R}^3$ is related to the COM position variation due to fuel burn. This vector is defined in terms of x, y, and z positions with respect to the COM in body reference frame.

Three reaction wheels (RWs), controlled by the onboard computer, are considered for the attitude control. A reaction wheel actuator can be modeled as a brushless motor attached to a high-inertia flywheel, which is free to spin along a fixed spacecraft axis. It produces a moment M_{RW}, causing its angular momentum to increase.

B. Position Mathematical Model

For circular orbits, and for the evaluation of the relative positions between two spacecraft, a local vertical local horizontal (LVLH) frame centered on the target vehicle is considered. In our case, the X axis V_{bar} is in the direction of the orbital velocity vector and the Y axis H_{bar} is in the opposite direction of the angular momentum vector of the orbit, whereas the Z axis R_{bar} is radial from the spacecraft centre of mass to the Earth center of mass as in Fig. 2.

Then, Hill's equations [16] are implemented to describe the relative motion of the two bodies in neighboring orbits:

$$\begin{aligned} \ddot{x} &= \frac{F_x}{m_c} + 2\omega\dot{z} \\ \ddot{y} &= \frac{F_y}{m_c} - \omega\dot{y} \\ \ddot{z} &= \frac{F_z}{m_c} - 2\omega\dot{x} + 3\omega^2 z \end{aligned} \tag{3}$$

where $x = [x, \dot{y}, z]^T \in \mathbb{R}^3$ is the position vector, $m_c \in \mathbb{R}$ is the chaser mass (known and varying with time), and $\omega \in \mathbb{R}$ is the angular frequency of the circular target (known and constant). The chaser mass varies, depending on the decrease of fuel mass, according to the model in [17]. $F = [F_x, F_y, F_z]^T \in \mathbb{R}^3$ is the total force vector, which is the sum of the forces due to the thrusters and the forces due to the action of the external environment disturbances affecting the system; that is,

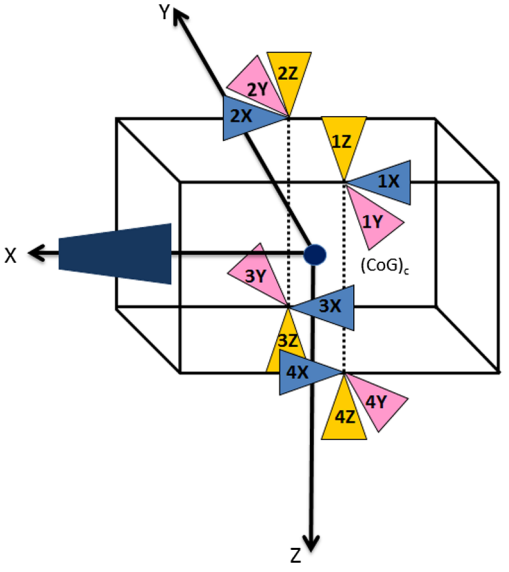

Forces	Thrusters	
+X	1X	3X
-X	2X	4X
+Y	2Y	3Y
-Y	1Y	4Y
+Z	3Z	4Z
-Z	2Z	1Z

Fig. 1 Thruster scheme on the spacecraft ($(CoG)_c$, chaser center of gravity).

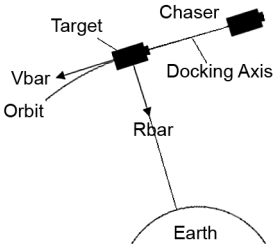

Fig. 2 LVLH frame definition.

$$F = F_{\text{thr}} + \Delta F_{\text{ex}} \tag{4}$$

where F_{thr} is given in Eq. (2); and $\Delta F_{\text{ex}} \in \mathbb{R}^3$ is the force associated to the action of the external disturbances, which is time varying. The force due to the thrusters is assumed to be affected by errors due to uncertainties in the shoot and magnitude of the thrusters, and they represent the control input designed according to the first-order sliding-mode methodology discussed in Sec. III.

The vector of forces obtained from the thrusters and the external disturbances is transformed from the body frame to the LVLH frame. Hence, we have

$$F = L_{\text{IB}} F^*$$

with $F^* \in \mathbb{R}^3$ as the force vector in the body frame (F_B frame; see Fig. 3), $F \in \mathbb{R}^3$ as the force vector in the LVLH frame [see Eq. (4)], and $L_{\text{IB}} \in \mathbb{R}^{3,3}$ the transformation matrix between the body and the LVLH frames.

The dynamics of the chaser position can be decomposed by considering the force due to the external disturbances, the thruster force, and the RW moment. Hence, system (3) can be rewritten as

$$\ddot{x} = A_x(x, \dot{x}) + \Delta_x + B_x u_x + \Delta_u \tag{5}$$

where $A_x(x, \dot{x}) \in \mathbb{R}^3$ is the nominal vector of the spacecraft dynamics, $\Delta_x = (1/m_c)\Delta F_{\text{ex}} \in \mathbb{R}^3$ is the vector collecting the uncertainties due to the external forces, $B_x = (1/m_c)I_3 \in \mathbb{R}^{3,3}$ is the control matrix, and m_c is the chaser mass. The input vector $u_x = F_{\text{thr}} \in \mathbb{R}^3$ [as in Eq. (2)] is designed with a sliding-mode controller, and $\Delta_u \in \mathbb{R}^3$ is the vector of thruster errors.

C. Euler and Kinematic Equations

For the evaluation of the spacecraft attitude angular velocities and angles, the Euler's moment equations and the kinematic equations are considered. The reference frame for these equations is the body reference frame, the origin of which is the center of mass of the spacecraft (see Fig. 3).

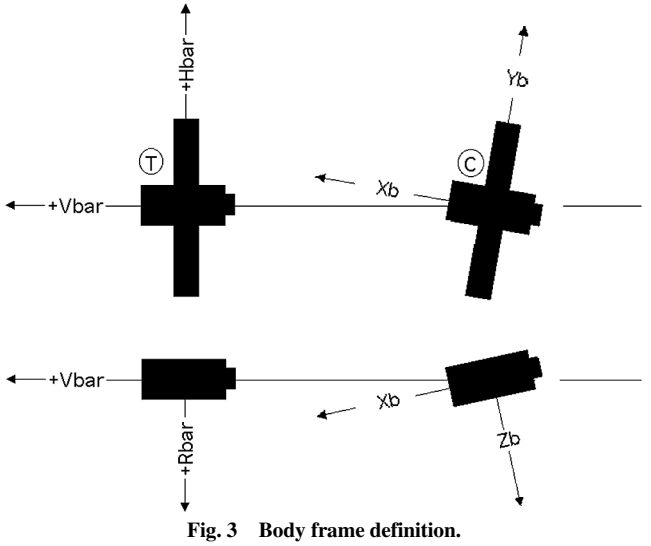

Fig. 3 Body frame definition.

The angular velocities are defined from the Euler equation as

$$\dot{\omega}_B = I^{-1}(M_B - \omega_B \times (I\omega_B + I_{\text{RW}}\omega_{\text{RW}})) \tag{6}$$

where $\omega_B = [p_B, q_B, r_B]^T \in \mathbb{R}^3$ is the vector of chaser angular velocities, I_{RW} is the RW moment of inertia (known and constant), and $\omega_{\text{RW}} = [\omega_{x,\text{RW}}, \omega_{y,\text{RW}}, \omega_{z,\text{RW}}]^T \in \mathbb{R}^3$ is the reaction wheel angular velocity. $M_B \in \mathbb{R}^3$ is the total moment acting on the chaser and is given by the sum

$$M_B = M_{\text{thr}} + \Delta M_{\text{ex}} + M_{\text{RW}}$$

where $\Delta M_{\text{ex}} \in \mathbb{R}^3$ is the moment due to the external disturbances. The body tensor $I \in \mathbb{R}^{3,3}$ of inertia is diagonal, and it is updated by taking into account the COM change of position.

With these quantities defined, system (6) can be rewritten as

$$\dot{\omega}_B = A_\omega(\omega_B, \omega_{\text{RW}}) + \Delta_\omega + \Delta_{\omega_{\text{thr}}} + B_\omega u_\omega \tag{7}$$

where $A(\omega_B, \omega_{\text{RW}}) \in \mathbb{R}^3$ is the vector of the angular velocity dynamics. The vector $\Delta_\omega = I^{-1}\Delta M_{\text{ex}} \in \mathbb{R}^3$ collects the uncertainties due to the external moments. The input vector u_ω is designed by a STW sliding-mode controller. The matrix $B_\omega = I^{-1} \in \mathbb{R}^{3,3}$ is the control matrix for the attitude control. $\Delta_{\omega_{\text{thr}}} = I^{-1}M_{\text{thr}} \in \mathbb{R}^3$ is the vector of uncertainties due to thruster moments.

Quaternions are used for the attitude evaluation

$$\dot{q} = \frac{1}{2}\Sigma(q)\omega_B \tag{8}$$

where $q = [q_1 q_2 q_3 q_4]^T \in \mathbb{R}^4$ is the vector of quaternions, and $\Sigma(q) \in \mathbb{R}^{4,3}$ is the quaternion matrix defined as

$$\Sigma(q)\begin{bmatrix} q_4 I_3 + Q_{13} \\ -q_{13}^T \end{bmatrix} \tag{9}$$

where $q_4 \in \mathbb{R}$ is the quaternion scalar component, $q_{13} \in \mathbb{R}^3$ is the vector of the first three components of the vector q, and $Q_{13} \in \mathbb{R}^{3,3}$ is the skew-symmetric matrix

$$Q_{13} = \begin{bmatrix} 0 & -q_3 & q_2 \\ q_3 & 0 & -q_1 \\ -q_2 & q_1 & 0 \end{bmatrix}$$

III. Sliding-Mode Strategies for Spacecraft Systems

As discussed in the Introduction (Sec. I), we propose two different sliding-mode controllers: 1) a first-order SMC for spacecraft position tracking, reducing the fuel consumption yet guaranteeing tracking in terms of positions and speeds; and 2) a STW SMC for the attitude control, including the quaternion dynamics.

A. Sliding-Mode Robustness to Uncertainties and Disturbances

The nonlinear dynamic model is affected by inaccuracies and uncertainties of various natures: in particular, parametric uncertainty (structured uncertainty) and unmodeled dynamics (unstructured uncertainty). Moreover, internal and external disturbances must be taken into account, which affect the system due to the real implementation and to the external environment. Sliding-mode methods provide controllers that are robust under large uncertainties. SMC can counteract uncertainties and disturbances, if the perturbations affecting the system are matched and bounded (first-order SMC) [8] or smooth matched disturbances with bounded gradients (second-order SMC) [9,10]. The case of unmatched bounded disturbances is more involved. Nevertheless, under some posed conditions, it can be dealt with by suitably designed SMC strategies [18–20].

B. Position Tracking SMC

For the position tracking, a first-order sliding mode is designed, motivated by the intrinsic nature of the thrusters, which cannot provide continuously modulated thrusts but can only be switched on and off. Indeed, the limited switching frequencies of the thrusters already pose serious feasibility issues to the implementation of a first-order SMC, considering both the fuel consumption and the capability to guarantee that the system trajectories reach and maintain a motion on the desired sliding manifold. To overcome these problems, we design a control strategy divided into two stages, which are identified mainly based on the chaser distance from the target and on different control switching parameters. In particular, the used control switching devices cannot be suitably exploited to sedisng a second-order sliding-mode algorithm [21]. However, it is important to emphasize that the adopted sliding output allows us to implement a first-order switching strategy that guarantees a strong reduction of fuel consumption.

The control vector u_x is designed according to the following first-order SMC law:

$$u_x = -B_x^{-1} K \mathrm{sgn}(\sigma_x) \tag{10}$$

where $B_x^{-1} = m_c(t) I_3$, $K = nT_{\max}$, and $n = 2$. This choice of n takes into account that two thrusters are turned on simultaneously to prevent moment misalignment (see the thruster scheme in Fig. 1). In general, the control gain K in Eq. (10) must guarantee that the sliding motion on the desired sliding manifold is reached and maintained. The designed sliding output σ_x, which is the switching function in the controller [Eq. (10)], is

$$\sigma_x = (\dot{x} - \dot{x}_d) + c_x(x - x_d) \tag{11}$$

where $\dot{x}_d$ and x_d are the vectors of the desired speed and the desired positions, respectively. The vectors of positions $x = [x, \dot{y}, z]^T$ and speeds $\dot{x} = [\dot{x}, \dot{y}, \dot{z}]^T$ are measured at each time step. The constant c_x is chosen positive. The desired sliding surface is $\sigma_x = 0$.

The desired positions $x_d = [x_d, \dot{y}_d, z_d]^T$ are assigned by considering that the chaser has to reach the target with their respective V_{bar} aligned. This means that the chaser has to move along the connection line between the two satellites. For the definition of the sliding surface, we require that, in the first part of the approaching phase ($x < 300$ m), the chaser should stay inside a defined cone with an assigned geometry (Fig. 4):

$$r_0 = 1 \text{ m}$$
$$r_f = 0.05 \text{ m}$$
$$\Delta h = \pm(x_f - x)\tan\theta + r_f$$

with $\theta = \arctan(r_0 - r_f/d)$. The desired z_d (along R_{bar}) is assigned step by step according to the actual chaser position, and it is equal to zero only when the chaser is 200 m ($x \geq 300$ m) from the target vehicle. The speed profile is chosen to have a descent ramp variation on $\dot{x}_d$ if $x \geq 300$ m and $\dot{y}_d = \dot{z}_d = 0$.

It should be remarked that the command u_x computed by the designed first-order SMC is discontinuous, and it is expected to switch infinitely fast. In practice, the control algorithm is computed at the same switching frequency of the thruster command. In this way, we can directly translate the (x, y, z) components of $u_x = [u_{x,1}, u_{x,2}, u_{x,3}]^T$ into the Boolean signal β defined in Eq. (1), assigning the on/off to thrusters. In particular, if we order the thrusters in Fig. 1 according to the sequence

$$\beta = \{1X, 3X, 2X, 4X, 2Y, 3Y, 1Y, 4Y, 3Z, 4Z, 1Z, 2Z\}$$

we obtain a specific algorithmic strategy for directly commanding the thruster. This is summarized in the Algorithm 1.

Algorithm 1. Thrusters switching algorithm

```
[Initialization]
  set f_x = 1 Hz, x = x_0 = [0,0,0]^T, ẋ = [V_x0, 0, 0]^T
[Control loop]
  while x < x_f, perform the following loop at frequency f_x
  [Desired positions and speeds]
    if x < 300
      set f_x = 1 Hz
      if |z| < |Δh|, set z_d = z
      else, set z_d = Δh
      set x_d = [x, 0, z_d] and ẋ_d = [V_x0, 0, 0]^T
    else
      set f_x = 20 Hz
      compute x_d = [x, 0, 0]^T and
              ẋ_d = [(V_x_f − V_x0/x_f − x_0)(x − x_i) + V_x0, 0, 0]^T
  [End of desired positions and speeds]
    end
  [Switching algorithm]
    compute σ_x according to Eq. (11)
    for i = 1 to 3
      β_4(i−1)+1 = 1/2 + (1/2)sgn(σ_x,i)
      β_4(i−1)+2 = 1/2 + (1/2)sgn(σ_x,i)
      β_4(i−1)+3 = 1/2 + (1/2)sgn(−σ_x,i)
      β_4(i−1)+4 = 1/2 + (1/2)sgn(−σ_x,i)
  [End of switching algorithm]
    end
  [Measurement]
    measure current position x and velocity ẋ
[End of control loop]
  end
```

C. Attitude Tracking SMC

For the tracking control problem of the attitude of the chaser, we consider a second-order sliding-mode algorithm [10]. The STW algorithm designs a continuous control law, which steers to zero in finite time both the sliding output and its first time derivative in the presence of smooth matched disturbances with bounded gradients, for which a bound is assumed to be known. The STW algorithm contains a term that is obtained as the integral of a discontinuous component. The chattering is not eliminated, yet it is strongly attenuated.

The input u_ω is defined in accordance with the STW algorithm [10] as follows:

$$u_\omega = -\lambda|\sigma_\omega|^{1/2}\mathrm{sgn}(\sigma_\omega) + v_\omega,$$
$$\dot{v}_\omega = \begin{cases} -u_\omega & \text{if } |u_\omega| > U_M, \\ -\alpha\,\mathrm{sgn}(\sigma_\omega) & \text{if } |u_\omega| \leq U_M \end{cases} \tag{12}$$

where the control parameters λ, α, and U_M have to be chosen as specified in [10].

The sliding output for the STW controller is defined as

$$\sigma_\omega = \omega_B + C_\omega \delta q_{13} \tag{13}$$

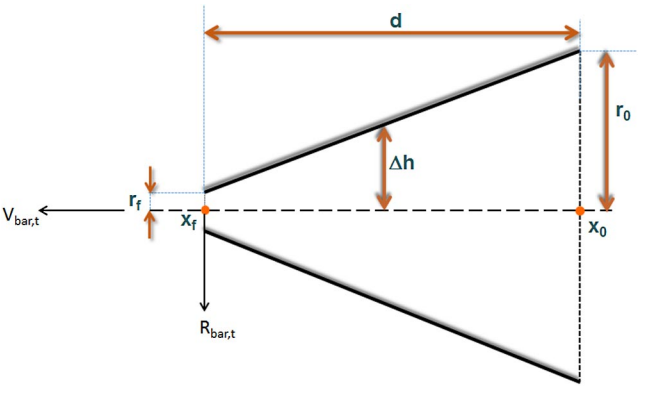

Fig. 4 Approaching maneuver cone geometry.

Table 1 Chaser and thruster characteristics

Parameter	Symbol	Unit
Initial mass	m_{c0}	600 kg
Initial inertia tensor	I_0	$144I_3$ kg · m^2
Zero shoot time of thrusters	t_{sp0}	0.02 s
Maximum thrust	T_{max}	1 N
Specific impulse of thrusters	I_{sp}	220 s
RW maximum torque	g_{max}	1 N · m
RW inertial tensor	I_{RW}	$0.1I_3$ kg · m^2

with $C_\omega \in \mathbb{R}^{3,3}$ as a positive definite matrix. The vector δq_{13} is evaluated starting from the desired attitude vector $q_d = [0 \quad 0 \quad 0 \quad 1]^T$, which means that the LVLH and body frames are aligned as

$$\delta q_{13} = \Sigma^T(q_d)q \tag{14}$$

where $\Sigma(q_d)$ is defined from the matrix $\Sigma(q)$ [Eq. (9)] including the q_d definition.

IV. Simulation Results

A six-degree-of-freedom simulation is considered to demonstrate the tracking performance of the proposed sliding-mode controller. Preliminary results related to the present work have been presented in [22], where a simplified three-degree-of-freedom model was addressed.

The simulation scenario assumes that the target center of mass is located at the origin of the LVLH reference frame and that it is 500 m ($x = 0$ m) from the chaser. The maneuver starts at point x_0 of Fig. 4 with a speed $V_{x0} = 0.15$ m/s at an orbit altitude of 650 km, which is the same orbit of the target. The maximum amplitude of the cone is $r_0 = 1$ m and the final R_{bar} is $r_f = 0.05$ m. The chaser has geometrical and inertial characteristics that are detailed in

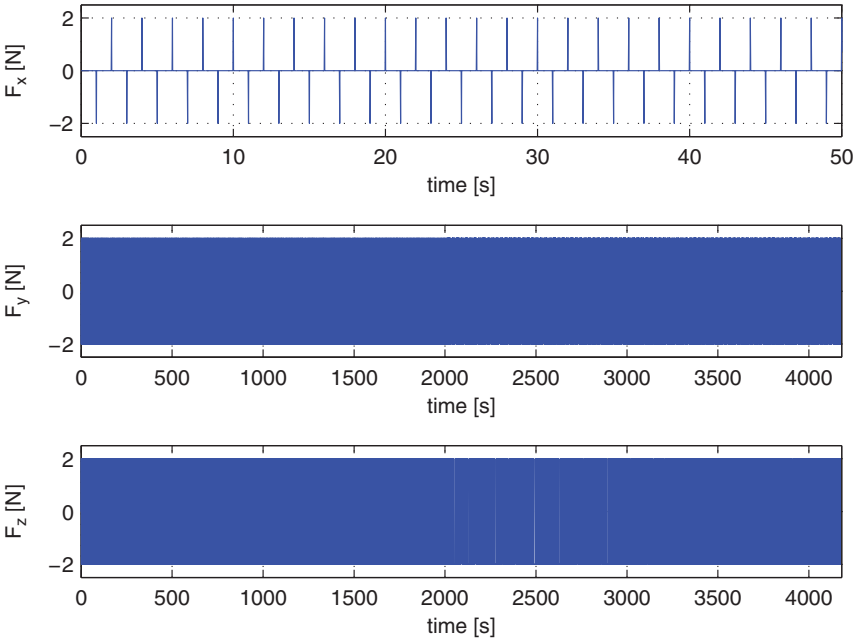

Fig. 5 Forces due to thrusters assigned by the first-order SMC.

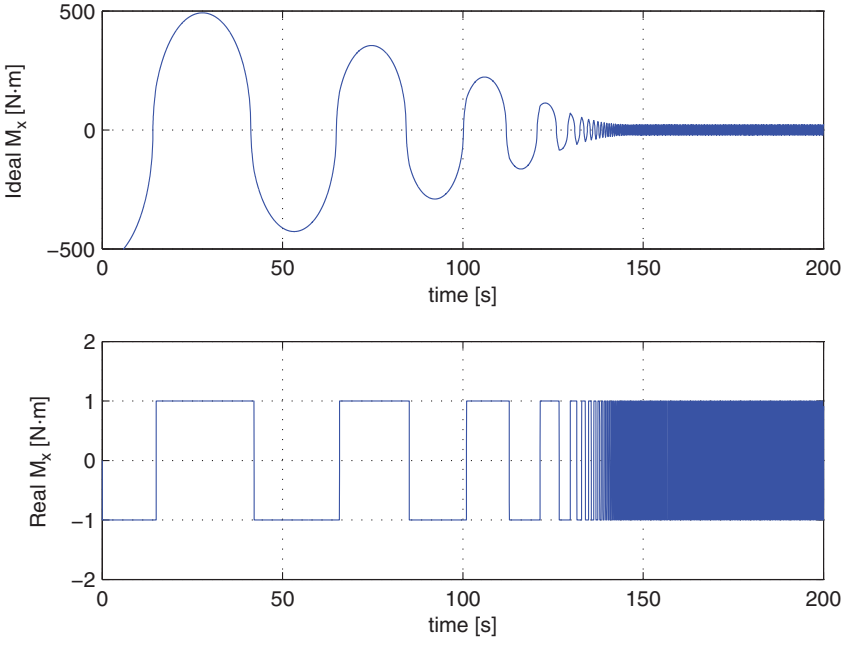

Fig. 6 Moment along *X* axis assigned by the STW SMC.

Table 2 Performance indicators

Case	Final R_{bar}	Fuel consumption	Total time
A	$z_f = 3.8 \cdot 10^{-4}$ m	$m_f = 3.072$ kg	$t_{\text{tot}} \cong 4172$ s
B	$z_f = 0.0091$ m	$m_f = 3.07$ kg	$t_{\text{tot}} \cong 4150$ s
C	$z_f = 0.0063$ m	$m_f = 1.56$ kg	$t_{\text{tot}} \cong 4145$ s

Table 1. In the simulations, the minimum feasible speed (imposed to the chaser vehicle) is $\dot{x}_f = 0.02$ m/s. The controller is switched off when the chaser is 2 m from the target (station-keeping point). The dynamics of the docking contact is not considered. For all the performed simulations, the initial quaternion vector is $q_0 = [0.42, 0, -0.1165, 0.9]^T$. The constant c_x of Eq. (11) is chosen equal to one. The geometry and inertial data for the orbiting modules are set by considering as reference the work of [23].

For the position SMC implementation, two frequencies at which the thrusters switch are considered as a function of the target–chaser distance along the V_{bar} axis are analyzed. In the first phase, when the chaser is far from the target ($x < 300$ m), a switching frequency of 1 Hz is selected. In the second phase ($x \geq 300$ m), a higher frequency f_x is chosen. In [22], different cases are analyzed, starting from $f_x = 1$ Hz to $f_x = 100$ Hz. Based on those preliminary results, and considering that, for real applications, control signals switching at high frequencies cannot be implemented, the following simulations are performed:

Case A: The second phase frequency is selected as $f_x = 50$ Hz. The sampling time of the simulation and the attitude controller (STW SMC) is equal to 100 Hz. No saturation and no filter are considered in the RW model. The system is affected by the errors of the thrusters and the disturbances due to the environment. The sampling time of the external disturbances is equal to 1 Hz. The sampling time of the thruster errors is equal to the switching frequency of the thrusters.

Case B: The second phase frequency is selected as $f_x = 20$ Hz. The sampling time of the simulation and the attitude controller is equal to 50 Hz. A real model for the reaction wheels is considered. The effects of the errors of the thrusters and the disturbances due to the environment are taken into account. The sampling time of the external disturbances is equal to 50 Hz. As in the previous cases, the sampling time of the thruster errors is equal to the switching frequency of the thrusters.

Case C: The sampling times for the position and attitude SMC controllers are as in Case B, where all the disturbances and a real model for the RWs are considered. To verify the effectiveness of the STW controller, a performance degradation of the controller is analyzed. We consider that the controller u_ω is equal to

$$\hat{u}_\omega = \rho u_\omega$$

with $\hat{u}_\omega$ as the "new" assigned control input in Eq. (12) and u_ω as the "old" control input. The degradation constant ρ varies from 1 to 0.6. This comparison is performed to validate the controller, even if one thruster is not working, and with a limited torque of the reaction wheels. The following case is analyzed of $\rho = 0.6$, where one thruster is switched off at $t = 1000$ s.

In Fig. 5, the thruster forces due to the position SMC are considered. For the variation along V_{bar} (plot on top), a zoom visualization of the first seconds of the simulations is shown, when the slow sampling time of 1 Hz can be observed. Note that, in this case, one does not get the usual infinitely fast oscillations typical of a SMC design. However, the produced trajectories are still satisfactory. In Fig. 6, the variation of the RW moment (along the X axis) due to the STW SMC is shown. The upper plot is the "ideal" moment assigned by the controller, whereas the lower plot is the actual moment assigned by the reaction wheels, taking into account the first-order filter and the saturation discussed in Sec. II.A. Note that the signal computed by the STW SMC (top) is indeed continuous, but it largely exceeds the maximum moment that can be obtained by the reaction wheels ($1 \cdot \text{N} \cdot \text{m}$). The moment actually applied to the wheels is in the bottom of Fig. 6.

The considered performance indicators (see Table 2) are the final R_{bar}, the fuel consumption, and the total time required to complete the docking maneuver. The obtained final R_{bar} has to be smaller than $r_f = 0.05$ m, which is the most important constraint to be satisfied to achieve the docking with the target.

For all the analyzed cases (see Fig. 7), even if the switching frequency of the position controller is lower in the first part of the path, the cone constraints are never violated. The best solution is obtained in case F_1; in fact, the r_f constraint is satisfied and a low fuel consumption is guaranteed. Moreover, even when the performances of the attitude controller are reduced with a degradation constant of $\rho = 0.6$, the quaternion vector (see Fig. 8) tracks the desired one in about 250 s; i.e., it is slower than the nominal case.

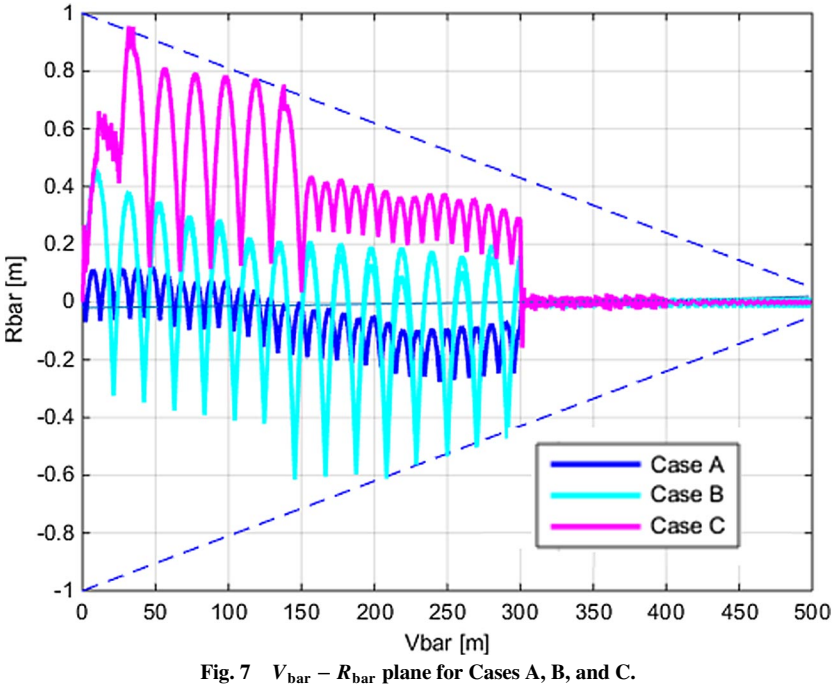

Fig. 7 $V_{\text{bar}} - R_{\text{bar}}$ plane for Cases A, B, and C.

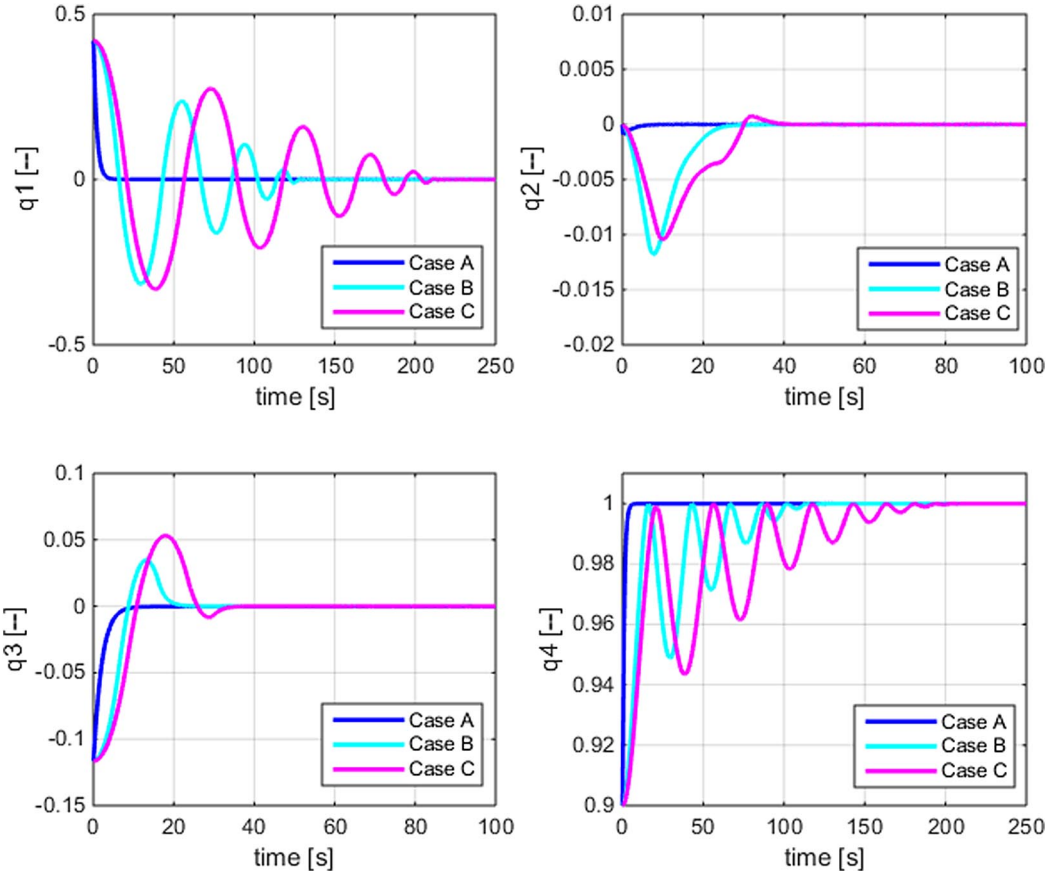

Fig. 8 Quaternions Cases A, B, and C.

V. Conclusions

This Note introduced different solutions based on sliding-mode controllers for simultaneous position tracking and attitude control of a docking maneuver between two spacecraft. For the position tracking, the proposed sliding-mode control (SMC) procedure considers different phases of the approaching maneuver, which are identified mainly based on the chaser distance from the target. The various stages correspond to different choices of the designed SMC switching parameters (different frequencies, gains, and desired velocity). For the attitude control, a second-order sliding mode, providing a continuous control signal to the reaction wheels, is designed. The simulation analysis shows that good performance of the controller is obtained even when the switching frequencies of the thrusters are low. Future directions of research will be focused on using second-order sliding-mode algorithms with adaptive gains for the attitude control; they will be mostly focused on exploiting advanced simplex SMC strategies, with the aim of deriving better shooting strategies and of developing position tracking systems that could be configurable in case of failures. This latter feature is of paramount importance to guarantee the success of the mission in the case of one or more thrusters malfunctioning.

References

[1] Dastidar, R. G., "On the Advantages and Limitations of Sliding Mode Control for Spacecraft," *AIAA Space Conference and Exposition*, AIAA Paper 2010-8777, 2010.

[2] Hughes, P. C., *Spacecraft Attitude Dynamics*, Dover, London, 2004, pp. 232–272, 480–520.

[3] Luo, W., Chu, Y. C., and Ling, K. V., "H_∞ Inverse Optimal Attitude-Tracking Control of Rigid Spacecraft," *Journal of Guidance, Control, and Dynamics*, Vol. 28, No. 3, 2005, pp. 481–493.

[4] Stansbery, D. T., and Cloutier, J. R., "Position and Attitude Control of a Spacecraft Using the State-Dependent Riccati Equation Technique," *Proceedings of the American Control Conference*, IEEE, Piscataway, NJ, 2000, pp. 1867–1871.

[5] Xin, M., and Pan, H., "Nonlinear Optimal Control of Spacecraft Approaching a Tumbling Target," *Proceedings of the American Control Conference*, IEEE, Piscataway, NJ, 2009, pp. 4818–4823.

[6] Subbarao, K., and Welsh, S., "Nonlinear Control of Motion Synchronization for Satellite Proximity Operations," *Journal of Guidance, Control, and Dynamics*, Vol. 31, No. 5, 2008, pp. 1284–1294.

[7] Weiss, A., Baldwin, M., Erwin, R. S., and Kolmanovsky, I., "Model Predictive Control for Spacecraft Rendezvous and Docking: Strategies for Handling Constraints and Case Studies," *IEEE Transactions on Control Systems Technology*, Vol. 23, No. 4, 2015, pp. 1638–1647.

[8] Utkin, V. I., *Sliding Modes in Optimization and Control Problems*, Springer, New York, 1992, pp. 189–205.

[9] Bartolini, G., Ferrara, A., and Usai, E., "Chattering Avoidance by Second-Order Sliding Mode Control," *IEEE Transactions on Automatic Control*, Vol. 43, No. 2, 1998, pp. 241–246.

[10] Levant, A., "Sliding Order and Sliding Accuracy in Sliding Mode Control," *International Journal of Control*, Vol. 58, No. 6, 1993, pp. 1247–1263.

[11] Tournes, C., Shtessel, Y., and Foreman, D., "Automatic Space Rendezvous and Docking Using Second Order Sliding Mode Control," *Sliding Mode Control*, edited by Bartoszewicz, A., InTech, Croatia, 2011, Chap. 16.

[12] Shtessel, Y. B., Tournes, C. H., and Fridman, L., "Special Issue On Advances in Guidance and Control of Aerospace Vehicles Using Sliding Mode Control and Observation Techniques," *Journal of the Franklin Institute*, Vol. 349, No. 2, 2012, pp. 391–396.

[13] Pukdeboon, C., and Kumam, P., "Robust Optimal Sliding Mode Control for Spacecraft Position and Attitude Maneuvers," *Aerospace Science and Technology*, Vol. 43, June 2015, pp. 329–342.

[14] Wilson, E., Sutter, D. W., and Mah, R. W., "Motion-Based Mass- and Thruster-Property Identification for Thruster-Controlled Spacecraft," *2005 AIAA Infotech@Aerospace Conference*, AIAA Paper 2005-6907, 2005.

[15] Wilson, E., Sutter, D. W., and Mah, R. W., "Motion-Based Thruster Fault Detection and Isolation," *Proceedings of the 2005 AIAA Infotech@Aerospace Conference*, AIAA Paper 2005-7182, 2005.

[16] Fehse, W., *Automated Rendezvous and Docking of Spacecraft*, Cambridge Univ. Press, New York, 2003, Chaps. 2, 3.

[17] Cornelisse, J. W., Schoyer, H. F. R., and Wakker, K. F., *Rocket Propulsion and Spacecraft Dynamics*, Pitman Publishing, London, 1979, Chap. 6.

[18] Cao, W. J., and Xu, J. X., "Nonlinear Integral-Type Sliding Surface for Both Matched and Unmatched Uncertain Systems," *IEEE Transactions on Automatic Control*, Vol. 49, No. 8, 2004, pp. 1355–1360.

[19] Castanos, F., and Fridman, L., "Analysis and Design of Integral Sliding Manifolds for Systems with Unmatched Perturbations," *IEEE Transactions on Automatic Control*, Vol. 51, No. 5, 2006, pp. 853–858.

[20] Mondal, S., Gokul, T. V., and Mahanta, C., "Adaptive Second Order Sliding Mode Controller for Vertical Take-Off and Landing Aircraft System," *IEEE 7th International Conference on Industrial and Information Systems (ICIIS)*, IEEE, Piscataway, NJ, 2012.

[21] Shtessel, Y., Edwards, C., and Fridman, L., *Sliding Mode Control and Observation*, Birkhauser, Springer, New York, 2014, pp. 143–182.

[22] Capello, E., Dabbene, F., Guglieri, G., Punta, E., and Tempo, R., "Rendezvous and Docking Position Tracking via Sliding Mode Control," *Proceedings of American Control Conference*, IEEE, Piscataway, NJ, 2015, pp. 1893–1898.

[23] Guglieri, G., Maroglio, F., Pellegrino, P., and Torre, L., "Design and Development of Guidance Navigation and Control Algorithms for Spacecraft Rendezvous and Docking Experimentation," *Acta Astronautica*, Vol. 94, No. 1, 2014, pp. 395–408.